Electron-Transfer Reactions in Organic Chemistry

Sebastião J. Formosinho[#] and Luís G. Arnaut*

Chemistry Department, University of Coimbra, 3049 Coimbra, Codex, Portugal

(Received February 19, 1996)

The Intersecting-State Model (ISM) is used to calculated the absolute rate constants of self-exchange electron-transfer reactions (ET) of organic species. The systems studied include aromatic hydrocarbons, quinones, nitrobenzene, aromatic nitriles, tetracyanoethylene, aromatic amines, and alkylhydrazines. All of the calculated rates are within one order of magnitude of the experimental ones, and the correlation coefficient between the two sets is 0.96. An electron-tunneling model has been developed to calculate distance-dependent nonadiabatic factors of intramolecular ET. This model can be used with ISM to calculate intramolecular ET rates. The system biphenylyl-spacer-naphthyl in tetrahydrofuran, whose distance-dependent intramolecular rates were measured by Closs and Miller, was used to test our calculations, because its ET rates can be calculated without adjustable parameters. Our absolute rate calculations are in an order-of-magnitude agreement with the experimental ones.

Electron-transfer processes (ET) are an important class of reactions in organic chemistry. Their relevance is particularly evident when one of the reactants is an organic radical or an electronically excited molecule. Then, the transfer of an electron to another organic molecule may be the dominant reaction path. Some practical applications of such processes have been summarized elsewhere.[1,2] ET reactions are also remarkable for their theoretical simplicity. The exchange of electrons between identical reactants and products is the simplest chemical reaction in a homogeneous solution, because it does not involve any bond-breaking or bond-forming process, and $\Delta G^\circ = 0$. Such electron self-exchanges can be represented by

$$ {}^*A^{Z_1} + A^{Z_2} \rightarrow {}^*A^{Z_2} + A^{Z_1} \qquad (1) $$

with $Z_2 - Z_1 = 1$, where Z_1 is the charge in a reduced form of species A and Z_2 the charge in an oxidized form of the same species; the asterisk is used only to distinguish between the otherwise identical species. Although electron self-exchanges have few practical consequences, they are of paramount importance in the development of theoretical models for ET reactions, and have been extensively studied, both theoretically and experimentally.

The electron-exchange rate between a radical ion and its parent molecule in a homogeneous solution is most conveniently measured using magnetic-resonance techniques. Depending on the nature of the solvent and counterions, the radicals may exist as free ions, ion pairs, or a mixture of both. This is particularly evident when sodium or potassium are used as reducing agents to form a radical ion from the neutral molecule. The electron-exchange rates are 2—3 orders of magnitude slower in tight ion pairs formed with alkali metal ions as counter ions, than in loose ion pairs.[3—5] An ion pair involving an alkali metal counterion,

$$ {}^*A^-M^+ + A \rightarrow {}^*A + A^-M^+, \qquad (2) $$

is a more complex system than that represented by mechanism (1). We are primarily interested in testing models that may lead to absolute estimates of the electron-exchange rates for the simplest organic systems. Thus, we focus attention on systems where tight ion pairs are not important. Experimentally, this normally corresponds to systems where the radical ions are produced by electrolysis in the presence of tetrabutylammonium iodide, tetrabutyl- or tetraethylammonium perchlorate as supporting electrolytes, or from dissociation in a solution of stable butylammonium or perchlorate salts. To have a consistent set of experimental electron-exchange rate constants to test the validity of theoretical models aimed at absolute rate-constant calculations, Table 1 was prepared with rates measured either in *N*,*N*-dimethylformamide (DMF) or in acetonitrile, because the static dielectric constants of these solvents are high and similar ($\varepsilon_s = 36.7$ and $\varepsilon_s = 35.94$, respectively). Furthermore, this table does not include data for systems involving simple changes of substituents, since at room temperature these lead to rate variations of less than a factor of 4;[6] i.e., benzonitrile is included, but methyl-substituted benzonitriles are omitted.[7]

Most theoretical approaches to the kinetics of the reactions illustrated by (1) are based on a theory developed by Marcus for inorganic ET reactions.[8—11] According to this theory, such reactions follow an outer-sphere mechanism, which postulates weakly bonded reactants (i.e. the electronic interaction between the reactants is less than 5 kJ mol^{-1}), and their rates can be calculated from

$$ k_{MT} = \varkappa_{el} Z \exp(-\Delta G^*/RT), \qquad (3) $$

where $\varkappa_{el}$ is a nonadiabatic factor ($\varkappa_{el} < 1$ for nonadiabatic

Also Universidade Católica Portuguesa, 3500 Viseu, Portugal.

Table 1. Experimental Data and Rate Constants Calculated According to ISM and Marcus Theory on Electron Self-Exchanges between Neutral Organic Molecules and Their Radical Ions

Reactants[a]	$n^{\ddagger}$ [b]	l_{ox} [c]	l_{red} [c]	f_{ox} [c]	f_{red} [c]	T	k_{ISM}	Solvent	k_{exp}	k_{MT}
		pm	pm	$J\,mol^{-1}\,pm^{-2}$	$J\,mol^{-1}\,pm^{-2}$	K	$M^{-1}\,s^{-1}$		$M^{-1}\,s^{-1}$	$M^{-1}\,s^{-1}$
Benzene$^{0/-}$	1.46	139.7[d]		387[d]		298	1.4×10^{9}			
Naphthalene$^{0/-}$	1.43	139.8[d]		381[d]		293	9.8×10^{8}	DMF	6.7×10^{8} [e]	1.9×10^{7} [f]
Anthracene$^{0/-}$	1.42	140.6[d]		377[d]		298	1.0×10^{9}	DMF	4.8×10^{8} [g]	4.2×10^{7} [f]
Biphenyl$^{0/-}$	1.44	139.9[h]		372[i]		298	1.6×10^{9}			
p-Benzoquinone$^{0/-}$	1.47	137.5[j]	138.5[k]	449[l]	429[m]	298	6.7×10^{8}	DMF	3.8×10^{8} [g]	6.3×10^{6} [f]
Nitrobenzene$^{0/-}$ [n]	1.375	120.8[o]		545[p]		298	3.0×10^{8}	DMF	3.0×10^{7} [g]	8.9×10^{6} [f]
TCNQ$^{0/-}$	1.73	134.4[q]	134.9[r]	525[s]	516[s]	293	3.2×10^{9}	AN	5.0×10^{9} [t]	1.4×10^{6} [u]
Tetracyanoethylene$^{0/-}$	1.97	130.1[v]	129.1[v]	642[w]	619[w]	293	8.7×10^{9}	AN	2.3×10^{9} [t]	1.5×10^{5} [u]
Benzonitrile$^{0/-}$	1.59	137.4[x]		445[y]		293	2.1×10^{9}	DMF	6.1×10^{8} [e]	7.5×10^{6} [f]
2,2′-Bipyridine$^{0/-}$	1.44	138.8[z]		376[aa]		298	1.6×10^{9}			
TMPPD$^{+/0}$	1.375	138.7[ab]	140.0[ac]	408[ad]	405[ad]	293	2.8×10^{8}	AN	1.2×10^{9} [t]	1.0×10^{6} [u]
PPD$^{+/0}$	1.375	138.3[ae]	139.1[ae]	403[af]	392[af]	293	3.7×10^{8}	AN	3.2×10^{8} [t]	4.8×10^{6} [ag]
DATCT$^{+/0}$	1.00	134.9[ah]	149.7[ah]	424[ai]	340[ai]	298	7.3×10^{4}	AN	1.2×10^{4} [aj]	5.0×10^{1} [ak]
Methyl viologen$^{2+/+}$	1.46	137.5[al]		401[al]		298	1.4×10^{9}			

a) TCNQ=7,7,8,8-tetracyano-*p*-quinodimethane; TMPPD=*N*,*N*,*N*′,*N*′-tetramethyl-*p*-phenylenediamine, PPD=*p*-phenylenediamine, DATCT=2,7-diazatetracyclo[6.2.2.2^{3,6}.0^{2,7}]tetradec-4-ene. b) Average bond order of the neutral and ion, calculated from Eq. 12 for exchanges with anions and given by Lewis structures for exchanges with cations. c) Representative bond lengths and force constants of the reactants, calculated as the average of all the bonds of the molecule or ion that participate in the reaction coordinate. d) Ref. 59, from naphthalene to naphthalene anion the frequencies of the skeletal carbon motions decrease by 10—30 cm^{-1}, indicating a 3% reduction in the force constants.[60] e) Ref. 7. f) Calculations done by Eberson[1] according to Marcus classical theory with neglect of the internal reorganization energy. g) Ref. 61. h) Ref. 62. i) Ref. 63. j) Ref. 64. k) Calculated with Gamess under the ROHF approximation.[65] l) Ref. 66. m) Estimated from the ratio of the frequencies of the neutral and anionic species.[67] n) Only the nitro group was considered to participate in the reaction coordinate. o) Ref. 68. p) Ref. 69. q) Ref. 70. r) Ref. 71. s) Ref. 72. t) Ref. 15. u) Calculation done by Grampp[15] using Marcus theory and accounting for inner- and outer-sphere reorganization energies. v) Ref. 73. w) Ref. 74. x) Ref. 75. y) Ref. 76. z) Ref. 77. aa) Ref. 78. ab) Ref. 46. ac) Ref. 79. ad) Ref. 80. ae) Ref. 25. af) Ref. 81. ag) Calculated using Marcus theory with the internal reorganization given by Clark[26] and the solvent reorganization given by Grampp,[50] as discussed in the text. ah) Ref. 47. ai) Using Gordy equation[82] calibrated with N–N bond date from *N*-nitrodimethylamine[83] and C–N single bond data from Ref. 84. aj) Ref. 14. ak) The internal reorganization energy (λ_i=82.7 $kJ\,mol^{-1}$) was estimated from the N–N bond changes only, using data in this table; the solvent reorganization energy (λ_o=129.4 $kJ\,mol^{-1}$) was calculated assuming that cation and neutral species have identical volumes with an average radius of 283.5 pm, estimated from their molecular dimensions in Ref. 14. al) Ref. 85.

exchanges), Z is the collision number of a bimolecular reaction in solution ($Z=10^{11}$ $M^{-1}\,s^{-1}$ at 298 K, M=mol dm^{-3})[1] and ΔG^{*} is the free energy of activation. When one of the reactants is a neutral molecule, there are only two contributions to ΔG^{*}, which are additive: the solvent (or outer-sphere) reorganization energy

$$\Delta G^{*}_{out} = \frac{e^2}{4}\left(\frac{1}{2r_{ox}}+\frac{1}{2r_{red}}-\frac{1}{r}\right)\left(\frac{1}{\varepsilon_{op}}-\frac{1}{\varepsilon_{s}}\right) \quad (4)$$

and the distortion of the reactant bonds on passing to the transition state (internal reorganization)

$$\Delta G^{*}_{in} = \sum_{j}\frac{f_j(R)f_j(P)}{f_j(R)+f_j(P)}[q_j(R)-q_j(P)]^2. \quad (5)$$

One of the most appealing features of the Marcus theory is its simplicity. The solvent reorganization energy can be calculated from the radii of the oxidized (r_{ox}) and reduced (r_{red}) reactants, their separation at the ET configuration ($r=r_{ox}+r_{red}$), and the optical (ε_{op}) and static (ε_{s}) dielectric constants of the solvent. The internal reorganization energy can be calculated from the force constants (f_j) of the jth vibrational coordinates in a species participating as reactant (R) and product (P), and the change $[q_j(R)-q_j(P)]$ in bond lengths and bond angles in going from reactant to product. However, electron exchanges in organic chemistry often involve flat aromatic molecules, for which the calculation of "effective" radii remains controversial. Several methods to estimate such radii have been proposed[12,13] and compared with more refined models which treat such flat aromatic molecules as oblate ellipsoids.[1,13] The latter models introduce some ambiguity in the distance between the reactants at the ET configuration, and are not convenient for performing the simple calculations, without adjustable parameters, needed to test the theory.

For a long time it was a strongly held belief that, in non-hydrogen-bonding solvents, the electron exchange between a large aromatic molecule and its radical ion involved only minor structural changes and, consequently, that the solvent reorganization was the dominant contribution to ΔG^{*}.[1,7] However, the ET reactivity in a series of increasingly larger polycyclic aromatic hydrocarbon anion radicals did not follow the size dependence expressed by Eq. 4, using either a spherical or a nonspherical model for the reactants.[13] Furthermore, the solvent dependence predicted by Eq. 4 was not confirmed in the detailed studies done by Nelsen,[14] Grampp,[15] and Bard.[16] Figure 1 presents a comparison between the observed solvent dependence of the electron self-exchange rates, with the predictions of Eq. 4 using the radii estimated by Eberson.[1] The rates presented are relative to the solvent

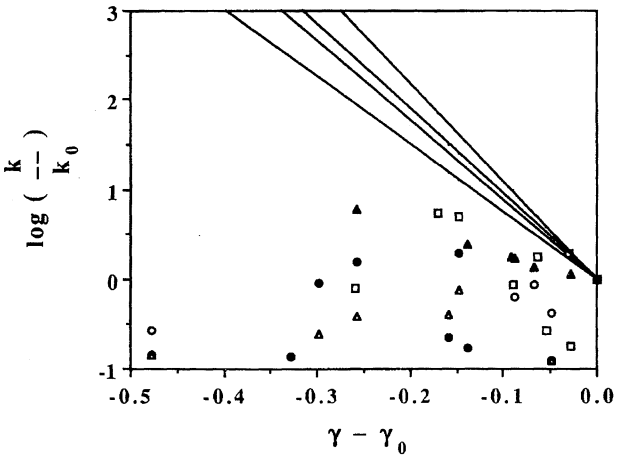

Fig. 1. Solvent dependence of self-exchanges of organic species as a function of the solvent parameter $\gamma=n_D^{-2}-\varepsilon^{-1}$. Filled triangles: TMPPD (r=820 pm); open triangles: TCNQ (r=820 pm); open circles benzonitrile (r=684 pm); filled circles: TCNE (r=650 pm); squares: DATCT (r=558 pm). The rates and solvent parameters are relative to the solvent with highest γ value, which Marcus theory predicts to give the slowest electron exchange rate. The lines were calculated with Eq. 4 for radii r estimated by Eberson, except for DATCT that is approximately spherical and crystal structure was employed to calculate r. See also Table 1 for the names of the compounds.

with the largest solvent parameter, $\gamma=n_D^{-2}-\varepsilon^{-1}$, which is predicted to yield the slowest rates. It is clear that these self-exchanges do not conform to the predictions of Eq. 4, and that the experimental rates are not strongly dependent on the solvent. Furthermore, Nelsen also showed that electron exchanges of several alkylhydrazines have similar energy barriers in acetonitrile and in the gas phase.[17] These and other solvent dependence studies[18] that do not conform to Eq. 4 lead to the suggestion that solvent dynamics could influence the dynamics of relatively slow ET reactions.[19,20] Although Barbara and co-workers[21] were able to provide convincing evidence for the influence of solvent dynamics in barrierless ET reactions, the nature and degree of dynamic effects in ET reactions with significant barriers remain open to some doubt.[22] The view emerging from recent experimental and theoretical information is that most self-exchange rates are only marginally influenced by changes in solvent identity,[23,24] and that internal reorganization is the major contributor to the activation barrier of many ET processes, leaving little room for solvent reorganization.[25,26]

The dominance of the internal reorganization in organic ET reactions raises questions concerning the applicability of the classical Marcus outer-sphere model to this type of reaction. The difficulties of the Marcus theory are even more evident in calculations of the reaction free-energy barriers by Eberson.[27] Using Eq. 4 and the effective radii for the reactants estimated from their molar volumes, this author calculated barriers that are some 10 kJ mol^{-1} higher than the experimental ones, even when the contribution from Eq. 5 is neglected. The contribution of the internal reorganization estimated by Grampp[15] for electron exchanges of aromatic molecules is ca. 5 kJ mol^{-1}. Adding these two contributions we calculated reaction rates that are three orders of magnitude slower than the experimental ones. Table 1 gives rate constants calculated by several authors using the Marcus theory (k_{MT}). A comparison between the calculated and experimental rates is illustrated in Fig. 2. Despite the simplicity of the systems represented by Eq. 1, it is evident that since the absolute rate calculations on these systems have not been very successful it would be desirable to have an alternative model.

In this work we present absolute rate calculations for electron self-exchange reactions of organic compounds using an alternative model, the Intersecting-State Model (ISM), that can be applied to reactions with variable degrees of electronic interaction between the reactants. We also introduce an electron-tunneling model to estimate the distance dependence of ET, and associate it with ISM in order to perform absolute rate constant calculations of intramolecular ET with $\Delta G^\circ \approx 0$. The rates calculated without adjustable parameters for the paradigmatic system biphenylyl-spacer-naphthyl in tetrahydrofuran, studied by Closs and Miller,[28] are within an order of magnitude of the experimental rates.

Theory of Bimolecular Organic Electron Transfers

The Intersecting-State Model has been described in detail in recent publications.[29—31] This model has been applied to ET reactions,[32—35] including absolute rate calculations of outer-sphere electron self-exchanges between transition-metal complexes in solution,[36,37] as well as to bond-breaking–bond-forming reactions.[38] ISM is based on the "diabatic reaction path" proposed by Evans and Polanyi.[39] The diabatic method to calculate activation energies consists in

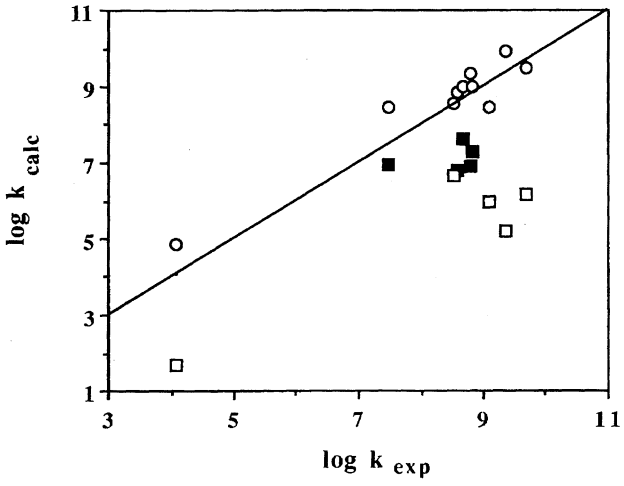

Fig. 2. Rate constants of the self-exchange ET shown in Table 1, calculated with ISM (circles) or Marcus theory (squares). Calculations using only the solvent reorganization energy given by Marcus theory are shown by open squares, and calculations also including the internal reorganization energy are shown by filled squares. The line represents the perfect correlation.

constructing two intersecting potential-energy surfaces, one representing the initial state and the other the final state of the reacting system, and then taking the cross-section through the two surfaces which leads to the lowest point of intersection between them.[40] In an example concerning a bond-breaking–bond-forming reaction, Polanyi centered these intersecting curves at the equilibrium geometries of reactant and product states.[41] The resonance energy between the initial and final states is treated as an additional factor.

In our application of ISM to bimolecular ET reactions, we considered that the reactants first approach each other to form the precursor complex, where the electron-transfer step may occur. The configuration of the activated complex in a nonradiative ET between the two reactants must obey the following two principles: i) the nuclear configuration of each species be identical in its oxidized and reduced forms; ii) the total electronic energy of the reactants be equal to that of the products. An activated complex configuration that meets the above criteria may be produced by the independent vibrations of the reactants in the precursor complex. Then, if the reactions are adiabatic ($\chi=1$), the electron is transferred and both species relax to their new equilibrium. Given that stretching force constants are much larger than the bending ones, and that an increase in the bond lengths decreases even further the bending force constants,[42] it is expected that the reaction coordinate is dominated by the stretching vibrations. The absence of large nonspecific solvent effects in the electron-exchange rates, and the theoretical expectation that solvent reorganization should require much less energy that bond stretches,[36] justifies, to a first approximation, the neglecting nonspecific solvent effects in those rates. This approximation may affect the calculated rates by a factor of five.

According to our model, the rate of passage through the activated complex configuration can be calculated with the transition state equation,

$$k = \chi \nu c_0^{1-m} \exp\left(-\frac{\Delta G^{\neq}}{RT}\right), \tag{6}$$

where ν is the frequency of conversion of the activated complex into products, χ is a transmission factor ($\chi=1$ for adiabatic and $\chi<1$ for nonadiabatic reactions), c_0 is the standard concentration ($c_0=1$ M), m is the molecularity of the reaction and $\Delta G^{\ddagger}$ is the free energy of activation. Given that the stretching vibrations dominate the reaction coordinate, the frequency (ν) is given by

$$\nu = \frac{k_B T}{h}. \tag{7}$$

Figure 3 illustrates the free-energy profile obtained for an electron exchange when a cross-section through the surfaces representing the initial and final states is taken along the diabatic path of the reactive stretching modes. The two reactants are represented by a single harmonic potential and characterized by a force constant (f_r), which is calculated as the average of the reactants force constants. The same is done for the two products. The free energy of activation

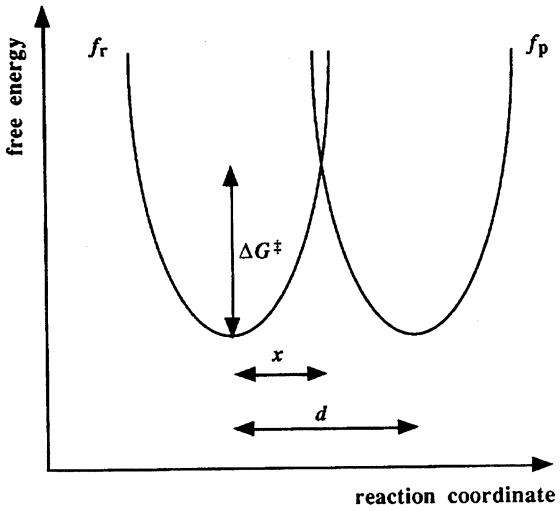

Fig. 3. Free energy profile along the reaction coordinate defined by ISM, where reactants and products are represented by harmonic oscillators of force constants f_r and f_p. The sum of the average bond distortion of the reactants with that of the products from their equilibrium configurations to the transition state one, is represented by the parameter d.

can be calculated if the displacement between the minima representing reactants and products (d) along the diabatic path is known,

$$\Delta G^{\ddagger} = \frac{1}{2}\frac{f_{red}+f_{ox}}{2}\left(\frac{d}{2}\right)^2. \tag{8}$$

According to ISM, that displacement is given by the sum of the effective bond distortions of the reactants and products from their equilibrium to their transition-state configurations,

$$d = (l_{ox}^{\ddagger} - l_{ox}) + (l_{red}^{\ddagger} - l_{red}), \tag{9}$$

where l_{ox} and l_{red} are the equilibrium bond lengths of the oxidized and reduced species. The bond distortions are expected to depend on their size (longer bonds may distort more than smaller bonds) and electron density (electronically rich bonds are more reluctant to change their lengths than single bonds). The relationship between the electron density and the bond length is conveniently addressed by Pauling's definition of bond order, which is valid for equilibrium structures. When $\Delta G^{\circ}=0$, the bond distortions along the diabatic path are given by[31,36,37]

$$d = \frac{a' \ln 2}{n^{\ddagger}}(l_{ox} + l_{red}), \tag{10}$$

where a' is an empirical constant (0.156) and $n^{\ddagger}$ is the transition-state bond order. The value of a' was obtained by fitting the energy barrier of the system $H+H_2$ calculated by ISM to that of rigorous potential energy surface calculations.[30]

Although maintaining the same theoretical framework, ISM offers a distinct treatment for bond-breaking–bond-forming and electron-transfer reactions. In the former, the reactants can be represented by the bond being broken and the products by the new bond formed. In the latter the two reactants (the organic molecule and the radical ion) must be

represented together, and the same must be done for the two products. Consequently, in the transfer of an electron the total bond order of the reactants is essentially preserved during the course of the reaction and $n^{\ddagger}$ is given by the average of the bond orders of molecule and its radical ion ($n^{\ddagger}_{av}$).

Using Eqs. 8 and 10, it is possible to calculate the activation free-energy of electron exchanges using the force constants, equilibrium bond lengths and valence bond orders. Inserting $\Delta G^{\ddagger}$ in Eq. 6 and taking the pre-exponential factor from Eq. 7, it is possible to calculate the bimolecular electron-exchange rate constants without adjustable parameters.

Since the ET between organic substrates usually involve many bonds, a criterion is needed to choose those that are relevant for the reaction coordinate. In order to establish such a criterion, it is convenient to rearrange Eqs. 8 and 10 to see more clearly how the reaction energy barrier depends on the parameters of the model. Replacing the constants by their values and using units of $J\,mol^{-1}\,pm^{-2}$ for the force constants and pm for the bond lengths, we obtain

$$\Delta G^{\ddagger} = 5.846 \times 10^{-3} \frac{1}{(n^{\ddagger}_{av})^2} f_{av} l^2_{av}, \tag{11}$$

where $n^{\ddagger}_{av}$, f_{av}, and l_{av} are the average values for the reduced and oxidized species. It follows from this expression that the reaction coordinate is not critically dependent on the force constants or bond lengths, because changes in l_{av} may be offset by opposing changes in f_{av}, as expressed by the well-known Badger rule.[43] However, it is particularly sensitive to the bond order, because $1 \leq n^{\ddagger}_{av} \leq 3$.

In the reduction of neutral aromatic molecules, the incoming electron is accommodated in a π^* molecular orbital. This antibonding orbital is delocalized over the aromatic system and leads to changes in the bond orders between the atoms it involves. Thus, the reaction coordinate used in ISM must account in an equitable manner for all of the bonds covered by the lowest unoccupied molecular orbital (LUMO) of the neutral molecule. The contribution of the C–H bonds to the reaction coordinate can be neglected. In that respect, nitrobenzene is a particular case, because in the anion the electron is localized on the nitro group;[44,45] therefore, only the NO bonds are included in the reaction coordinate.

In the oxidation of aromatic amines, an electron is removed from the nitrogen nonbonding orbital. PPP calculations on *N,N,N′,N′*-tetramethyl-*p*-phenylenediamine (TMPPD) show that the π bond orders of the molecule change upon oxidation by values ranging from 7% (central CC bond of the aromatic ring) to 14% (Ar–N bond).[46] Thus, all bonds of the aromatic ring and its bonds with the nitrogen atoms must be accounted for in the reaction coordinate. Only the C–H and N–CH_3 bonds are left out. In the oxidation of alkylhydrazines an electron is also removed from the nitrogen non-bonding orbital. The X-ray structures show that it is the N–N bond that is more critically perturbed in the course of the oxidation,[47] and the reaction coordinate is considered to be dominated by this bond.

Now that the bonds contributing to the reaction coordinate in a concerted way have been selected, the unidimensional nature of ISM requires that a method is devised to combine them into a single effective bond, characterized by a set of parameters: $n^{\ddagger}$, f, and l. Taking the average of the values of those bonds is the simplest and most equitable way of achieving this. The averages obtained for the oxidized and reduced species are shown in Table 1. When available, we selected "experimental" force constants obtained from the valence force fields using normal coordinate calculations to reproduce vibrational frequencies, bond lengths determined by X-ray measurements, and bond orders from simple valence structures of the neutral and radical species. The decrease in the bond order of an aromatic anionic radical with an electron in a π^* molecular orbital relative to the bond order of the corresponding neutral molecules can be estimated from

$$\Delta n^{\ddagger}_{a} = -\frac{0.5}{n_b}, \tag{12}$$

where n_b is the number of bonds included in the reaction coordinate. For example, since tetracyanoethylene has four triple bonds, four single bonds and one double bond, its average bond order is 2.00; from Eq. 12 its anion has an average bond order of 1.94 and, consequently, the transition state bond order for the electron exchange is 1.97. Since the radical cations considered in this work are formed by removing an electron from a nitrogen nonbonding orbital, their bond orders are considered to be equal to those of the corresponding molecules.

Relatively few values for the force constants and bond lengths of organic radicals have been determined experimentally. The values shown in Table 1 can be used to test the compensating effects of the bond length and force-constant changes with ET. Calculations using only the force constants and bond lengths for the neutral molecules give rate constants that differ by less than 20% from those using also the data from the radicals.

A comparison between the equations of Marcus theory and those used by ISM reveals that they lead to different transition-state configurations and, consequently, that they correspond to different reactivity models. There are two major differences between these models. The Marcus theory predicts that the solvent reorganization is the dominant contribution to the ET energy barrier in polar solvents, while ISM considers that the solvent can only dominate the kinetics of very fast reactions. The Marcus theory locates the transition state for the internal reorganization of each reactive bond somewhere in between its length in the reduced and oxidized form, while ISM uses a diabatic path subject to the condition of bond-order conservation to locate that transition state for an outer-sphere ET reaction, giving $l^{\ddagger} > l_{ox}, l_{red}$.

Furthermore, there is a controversy concerning the mechanism of the reactions represented by Eq. 1: They either follow an outer-sphere mechanism and the Marcus theory can be employed, or they follow an inner-sphere mechanism, as recently suggested by Shaik, and involve a signifficant resonance at the transition state.[27,48] Actually, the distinction between inner- and outer-sphere ET reactions is a matter of

degree of the electronic interaction, and only long-range ET between distant redox centers would be a truly outer-sphere process.[49] It is more satisfactory to approach the mechanistic continuum from purely outer- to predominantely inner-sphere ET reactions using a model that can be employed to calculate the rates of both types of reactions, as is the case of ISM.

Results of Calculations on Electron Self-Exchanges

Table 1 presents the experimental parameters used by ISM to calculate electron-exchange rates with Eqs. 11, 7, and 6 under the assumption that the reactions are adiabatic (χ=1). This assumption should be verified in bimolecular electron-exchanges of organic species in solution, because the electron is exchanged between orbitals of the same symmetry and reactants in close contact (center-to-center distance of 300 to 400 pm in a sandwich-like arrangement). It is important to emphasize that ISM is used here to calculate the *absolute* rates. By "absolute" we mean that, once the approximations of the model are defined, *no parameters are adjusted.* The quality of the obtained results can be best appreciated in Fig. 2, where the experimental rates are compared with the rates calculated with ISM or the Marcus theory. The relationship between the experimental rates and the rates calculated with ISM has a correlation coefficient of 0.96. There is no correlation with calculations using the Marcus theory at the same level of sophistication, that is, using the dielectric continuum approximation and representing the reactants by spheres with an effective radius. Inclusion of the internal reorganization energy in the calculations with the Marcus theory leads, in all cases, to very large discrepancies with the experimental values. A paradigmatic example is the electron exchange between *p*-phenylenediamine (PPD) and its radical anion. The internal reorganization energy of this couple in the gas phase was calculated by Rauhut and Clark using molecular-orbital methods. At 300 K they obtained ΔG^{*}_{in}=14.4 kJ mol^{-1}.[26] On the other hand, Grampp estimated ΔG^{*}_{out}=9.8 kJ mol^{-1} in acetonitrile.[50] Using Marcus theory with $Z=10^{11}$ M^{-1} s^{-1} and $\varkappa_{el}$=1, we calculated $k_{MT}=4.8\times10^{6}$ M^{-1} s^{-1} at 293 K. The experimental rate is 3.2×10^{8} M^{-1} s^{-1}. The rate calculated by ISM is 3.7×10^{8} M^{-1} s^{-1}.

It was mentioned in the Introduction that the rate constants for mechanism (2) are 2—3 orders of magnitude slower than for mechanism (1). This can be rationalized in terms of ISM simply by considering that the alkali metal counter ion withdraws some electronic density from the reaction coordinate, thus reducing the value of $n^{\ddagger}$. A 13% decrease in $n^{\ddagger}$, from 1.43 to 1.24, reproduces the experimental rate constant for the electron exchange between naphthalene and naphthalenide in THF with K^{+} as counterion (6×10^{7} M^{-1} s^{-1}). This value of $n^{\ddagger}$ corresponds to the average between the typical bond order of the neutral molecule and a bond order of unity for the radical anion in the ion pair, indicating that the π-electron density in the ion pair is withdrawn from the reaction coordinate due to the Coulombic attraction by the alkali metal. A ca. 13% decrease in $n^{\ddagger}$ had also been found in the deprotonation of toluene by cesium versus lithium cyclohexylamine, which was assigned to a strong interaction between the lithium and the reactants in the ion pair.[51] The physically meaningful variation of the parameter $n^{\ddagger}$ gives support to the utilization of ISM to interpret data in more complex systems where absolute rate calculations are difficult to perform.

Theory of Intramolecular Electron Transfer

The transfer of an electron from a donor to a covalently linked acceptor across a rigid spacer, became one of the central themes in the field of ET following the seminal work of Closs and Miller.[28,52] ISM can also be applied to calculate the ET rate constants in such systems, provided that a model is designed to estimate the distance dependence of the ET rate constants. In this section we develop the foundations of such a model.

Donor and acceptor are considered to be held rigidly apart at well-defined distances. We can picture this system considering that the donor is a box containing a "free electron", separated by a rigid bridge from the acceptor, which is a lower energy box. This bridge has the properties of a dielectric, because it is polarizable and because the electron does not have enough energy to escape its initial box through the conduction band of the bridge. Thus, the electron can only be transmitted to the lower energy box by tunneling. To further simplify the system, the boxes are considered to be unidimensional with their orientation collinear with the bridge. The size of the tunneling barrier is determined by the length of the bridge. The height of the barrier can be approximated by the difference between the energy of the electron in the donor box and the energy that it would experience in the dielectric. In this simple formulation, the tunneling barrier is rectangular and the effect of the relative orientation of the different parts of the system is not considered.

The frequency of the movement of the electron in its box can be estimated from the zero-point energy of a particle in a potential well of infinite walls and from the relation $E=h\nu$, which give

$$\nu=\frac{h}{8m_e(\Delta r)^2}, \tag{13}$$

where m_e is the mass of the electron and Δr the size of the unidimensional well. If we take Δr as the length of the two aromatic rings of naphthalene, which is approximately 480 pm if the CH bonds are excluded, we obtain $\nu=4\times10^{14}$ s^{-1}. This is in good agreement with the frequency factors used in ET processes involving electron donors similar to those considered here, that are in the range 10^{14}—10^{15} s^{-1}.[53,54] In our calculations of intramolecular ET was used $\nu=5\times10^{14}$ s^{-1}.

The permeability of a rectangular barrier of height Φ to a particle of mass m_e is given, according to the WKB approximation, by

$$\chi=\exp\left\{-\frac{4\pi}{h}\sqrt{2m_e\Phi}r\right\}=\exp\{-\beta r\}, \tag{14}$$

where r is the length of the barrier and β is the tunneling

decay coefficient. The parameter r is given by the edge-to-edge distance between the box of the donor and that of the acceptor. This parameter can be taken from the geometry of each particular system. In order to calculate the height of the barrier it is necessary to estimate the energy of the electron in the donor and its virtual energy in the dielectric.

The energy of the electron in the HOMO of a radical anion relative to its energy in a reference electrode is given by its reduction potential. This energy depends on the solvent. Many electrochemical potentials have been measured against a saturated aqueous calomel reference electrode (SCE). On the other hand, we can use the absolute potential of SCE selected by Heinis, $E_{red}=-4.71$ eV,[55] to obtain the energy of the electron in the box relative to its energy in the vacuum at infinite separation from the donor and zero kinetic energy. Figure 4 illustrates how these calculations can be made.

The energy of the electron in the bridge can, in principle, be estimated in the same way. However, the reduction potentials of bridges made of saturated hydrocarbon chains cannot be determined in acetonitrile. The gas-phase electron affinities of such molecules indicate that their LUMO is located more than 4 eV above the energy of the electron in a vacuum.[56] Although the energy of the LUMO is stabilized by the solvent, estimates of such stabilization are not very reliable. Thus, it is not possible to have a direct measure of the energy of the electron in a bridge made of an aliphatic hydrocarbon.

This problem can be addressed in a different manner. The Coulomb potential energy of one charge (q) at a distance r from another charge (q') in the vacuum is given by

$$\Phi_0 = \frac{1}{4\pi\varepsilon_0}\frac{qq'}{r}, \tag{15}$$

where ε_0 is the permitivity of the vacuum. If the vacuum is replaced by a medium of permitivity $\varepsilon=\varepsilon_r\varepsilon_0$, where ε_r is the relative permitivity (or dielectric constant) of the medium,

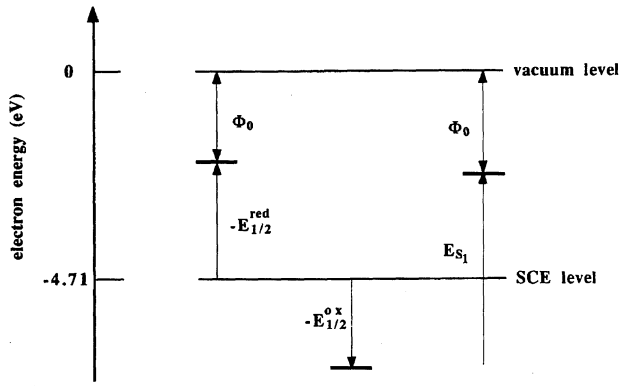

Fig. 4. Schematic representation of the energy of one electron in a radical anion (left), radical cation (center) or electronically excited molecule (right), relative to its potential energy in the vacuum at infinite separation from the radical ion. The relative energy of the electron in the SCE is shown to define the energy scale. The energies of the electron reflect those of biphenyl in different oxidation or electronic states, using data from Table 2.

$$\Phi_r = \frac{1}{4\pi\varepsilon_r\varepsilon_0}\frac{qq'}{r}. \tag{16}$$

For those charges at the same distance, these potentials are related by

$$\Phi_r = \frac{\Phi_0}{\varepsilon_r}. \tag{17}$$

The calculations performed according to Fig. 4 give the energy of the electron in the box relative to its energy in the vacuum. In order to correct for the effect of the dielectric separating donor and acceptor, and to obtain the virtual potential energy barrier for the transfer of the electron through the bridge, it is necessary to use Eq. 17. However, static dielectric constants should not be used in Eq. 17, because the frequency of electron movement in a molecule is very high. For high frequencies it is more appropriate to model the medium by its optical dielectric constant, which can be approximated by the square of its refractive index (n_D). The frequency of the electron movement estimated by Eq. 13 is very close to the frequency of the sodium vapor D line, 5.0×10^{14} s^{-1}, which lends support to the use of the refractive index in Eq. 17. Thus, this equation can be rewritten as

$$\Phi_r = \frac{\Phi_0}{n_D^2}. \tag{18}$$

The particularity of this tunneling model is to account for the stabilization of the energy of the electron in the bridge, by considering the dielectric properties of the bridge.

We can now follow a scheme similar to that of Fig. 4 and associate it with Eq. 18 to obtain the energy barrier to be used in Eq. 14. That is, we calculate the tunneling decay coefficients making $\Phi=\Phi_r$. Representative results are given in Table 2 and illustrated in Fig. 5. The distance r that appears in Eq. 14 is taken from the experimental geometry of the system. Such calculations give the distance dependence of intramolecular electron transfers. The frequency of such

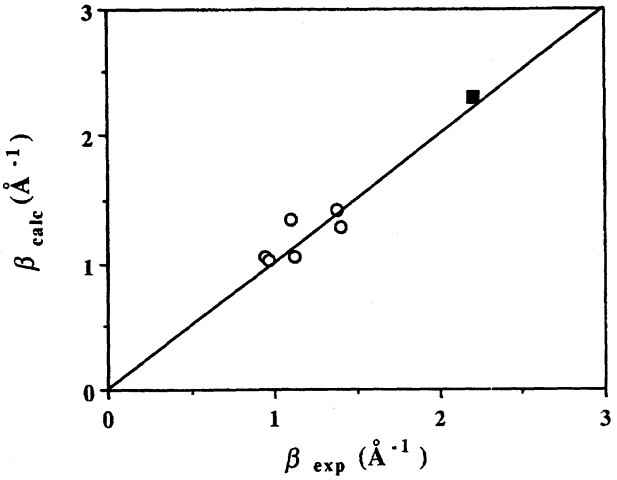

Fig. 5. Correlation between calculated and experimental tunneling decay coefficients, using data from Table 2. The correlation coefficient is 0.97. The circles represent intramolecular ET and the square is the electron tunneling through vacuum. The line represents the perfect correlation.

Table 2. Electrochemical Potentials, Singlet Excited State Energies of Electron Donors and Tunneling Decay Coefficients in Intramolecular ET [a)]

Donor	Spacer	$E^{red}_{1/2}$	$E^{ox}_{1/2}$	E_{S_1}	Φ [b)]	β_{calcd}	Solvent	β_{exp}
		eV	eV	eV	eV	Å^{-1}		Å^{-1}
Biphenyl$^-$	Cyclohexylene	−2.58[c)]	1.91[c)]	4.16[c)]	1.07	1.06	THF	1.12[d)]
Biphenyl$^-$	Cubanediyl	−2.58[c)]	1.91[c)]	4.16[c)]	1.07	1.06	THF	0.94[e)]
Dimethoxynaphthalene*	Polynorbornanediyl		1.1[f)]	3.78[f)]	1.015	1.03	THF	0.96[f)]
$Ru^{2+}(bpy)^*_3$	$-CH_2-$		1.22[g)]	2.08[g)]	1.925	1.42	Acetonitrile	1.38[g)]
ZnTTP* [h)]	Oligospirocyclobutanediyl		0.75[h)]	2.01[h)]	1.725	1.34	Acetonitrile	1.1[h)]
ZnPAP* [i)]	Bicyclo[2.2.2]octanediyl		0.59[i)]	2.15[i)]	1.58	1.29	Acetonitrile	1.4[i)]

a) Electrochemical potentials measured against SCE. b) Calculated using n_D^2=2.0 and Eq. 17. c) Ref. 86. d) From the edge-to-edge distance between donor and acceptor in equatorial positions in Ref. 28. e) From the center-to-center distance between donor and acceptor in Ref. 87. f) Ref. 88. g) Ref. 89. h) (5,10,15,20-Tetra-*p*-tolylporphyrinato)zinc from data in Ref. 90, using edge-to-edge distance. i) (2,3,7,8,12,13,17,18-Octamethyl-5,10,15,20-tetraphenylporphyrinato)zinc from data in Ref. 91, using center-to-center distance.

transfers can be given by Eq. 13. The free-energy barrier for the electron transfers can be calculated from Eq. 11 if $\Delta G^\circ \approx 0$. Finally, knowing the frequency, the permeability and the free-energy barrier, Eq. 6 can be employed to provide *absolute* calculations of the electron-transfer rate constants as a function of the distance between the donor and acceptor.

The frequency employed for intermolecular electron-exchanges at room temperature (Eq. 7) is two orders of magnitude lower than the frequency employed for intramolecular reactions (5×10^{14} s^{-1}). It is interesting to note that the nonadiabatic factor expected for an intramolecular ET occurring at a donor-acceptor distance of 3.5 Å and with the typical tunneling decay coefficients of Table 2, is comparable to the difference in frequency factors between inter and intramolecular exchanges. This suggests that the nuclear frequency becomes the dominant frequency factor of intermolecular electron exchanges due to a decrease in the product of the electronic frequency with its associated distance-dependent factor.

Results of Calculations on Intramolecular Electron Transfers

Table 2 presents the experimental and calculated tunneling decay coefficients of some intramolecular ET. The data selected include all systems with saturated hydrocarbons as spacers for which an approximately linear donor-spacer-acceptor orientation exists and for which the ET rate constants were determined as a function of the distance. The decay coefficient of tunneling through a vacuum, determined by Binning et al.[57,58] in the development of the scanning tunneling microscope, was also included. Our calculations employed Eqs. 18 and 14; the height of the tunneling barrier was calculated using the electrochemical potentials and the excited state energies presented in the table. In Fig. 5 we present the relationship between the calculated and experimental coefficients. The correlation coefficient between the two sets of coefficients is 0.97, including the data on tunneling through a vacuum.

The quality of the correlation presented in Fig. 5 gives support to the use of Eq. 18 to calculate the height of the tunneling barrier, together with approximation of this barrier to a rectangular shape. The simplifications involved in the development of the tunneling model do not allow, at this stage, a refinement of the theory to account for the orientational effects of the systems. Such effects may produce one-order-of-magnitude variations in the rates.

In our calculations we considered that n_D^2 is constant for all the saturated hydrocarbon spacers, and set its value equal to 2. Actually, it is well-known that the refractive index increases with the chain length in a series of saturated hydrocarbon molecules. For example, although pentane has n_D^2=1.84, for nonane n_D^2=1.98. The impact of these changes on n_D in the calculation of β is small. Such changes lead, for the systems studied by Closs and Miller, to a range of β values from 1.10 to 1.06. The experimental value is 1.12.[28]

The success of ISM in the calculation of the absolute self-exchange ET rate constants and of the tunneling model to calculate the absolute tunneling decay coefficients, encourages us to perform absolute calculations of intramolecular ET when $\Delta G^\circ \approx 0$. A most appropriate test for our model is the distance-dependent rate constants of the paradigmatic system biphenylyl-spacer-naphthyl in tetrahydrofuran, studied by Closs and Miller, because $|\Delta G^\circ| \leq 0.05$ eV.[28] The spacers used were cyclohexane, trans-decalin or a steroid; only stereoisomers in equatorial positions were considered. The parameters employed in these calculations were taken from Table 1, and treated in the same manner as for the self-exchange reactions. Using the data for biphenyl and naphthalene, we obtained $f_r=f_p=376.5$ J mol^{-1} pm^{-2}, $l_{red}+l_{ox}=279.7$ pm, and $n^\ddagger=1.435$. The tunneling decay coefficient can be taken from Table 2, $\beta=1.06$ Å^{-1}, the frequency factor, based on Eq. 13, was set as 5×10^{14} s^{-1}, and the distances between donor and acceptor are the edge-to-edge distances given by the geometry of the systems. As shown in Fig. 6, our *absolute* rate-constant calculations for intramolecular ET are within an order of magnitude of the experimental ones, and reproduce their distance dependence.

Conclusions

We applied ISM to calculation of the rate constants of a large variety of electron self-exchange reactions involving organic species. The reaction coordinate involves the bonds participating in the molecular orbital where the electron being transferred is initially located. Averages of the

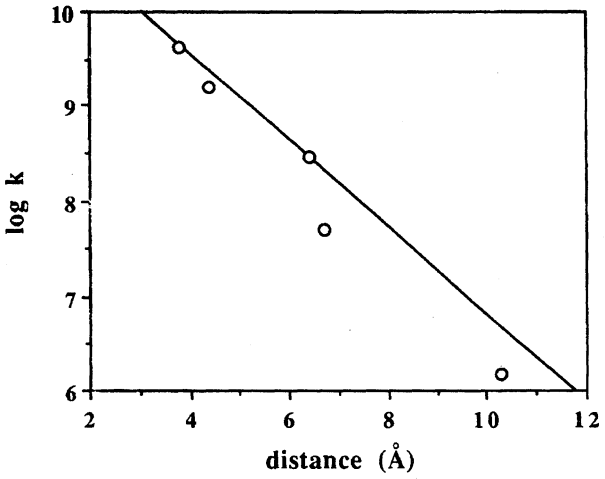

Fig. 6. Experimental (circles) and calculated (line) intramolecular ET from the biphenylyl anion to naphthyl, across cyclohexane, *trans*-decalin or steroid spacers. Only experimental rate constants and edge-to-edge distances concerning donor and acceptor in equatorial positions are shown. All the parameters used in the calculations were taken from biphenyl and naphthalene in Table 1.

force constants, bond lengths and bond orders of the bonds between these atoms provide the parameters used in ISM. With these parameters, it is possible to calculate rate constants that are within a factor of ten of the experimental values. No parameters were adjusted in our calculations. A comparison between our calculations and those following the Marcus theory, reveals that ISM is a signifficant improvement in the ability to predict electron self-exchange rates in organic chemistry.

Intramolecular ET rate constants of organic systems where $\Delta G^\circ \approx 0$ can also be calculated in the same manner if the distance-dependent nonadiabatic factor is calculated independently. A tunneling model to calculate such a factor was proposed, based on electron tunneling through a square energy barrier. The length of this barrier is given by the edge-to-edge separation of the donor and acceptor groups. Its height is given by the difference in energy of the electron in the donor and its energy in the dielectric that separates the donor from the acceptor. By associating this tunneling model with ISM it is possible to calculate intramolecular ET rate constants without adjusting any parameters, provided that $\Delta G^\circ \approx 0$.

The authors acknowledge Junta Nacional de Investigação Científica e Tecnológica and PRAXIS XXI Programme for financial support of this research.

References

1) L. Eberson, *Adv. Phys. Org. Chem.*, **18**, 79 (1982).
2) L. G. Arnaut, *J. Photochem. Photobiol. A: Chem.*, **82**, vii (1994).
3) R. Chang and C. S. Johnson, Jr., *J. Am. Chem. Soc.*, **88**, 2338 (1966).
4) N. Hirota, R. Carraway, and W. Schook, *J. Am. Chem. Soc.*, **90**, 3611 (1968).
5) C. L. Malinoski, Jr., W. H. Bruning, and R. G. Griffin, *J. Am. Chem. Soc.*, **92**, 2665 (1970).
6) M. Goez, *Z. Physik. Chem. N. F.*, **169**, 123 (1990).
7) H. Kojima and A. J. Bard, *J. Am. Chem. Soc.*, **97**, 6317 (1975).
8) R. A. Marcus, *J. Chem. Phys.*, **24**, 966 (1956).
9) R. A. Marcus, *J. Chem. Phys.*, **26**, 867 (1957).
10) R. A. Marcus, *Faraday Discuss. Chem. Soc.*, **29**, 21 (1960).
11) R. A. Marcus, *J. Chem. Phys.*, **43**, 679 (1965).
12) M. E. Peover, *Electrochim. Acta*, **13**, 1083 (1968).
13) K. Suga, S. Ishikawa, and S. Aoyagui, *Bull. Chem. Soc. Jpn.*, **46**, 808 (1973).
14) S. F. Nelsen, Y. Kim, and S. C. Blackstock, *J. Am. Chem. Soc.*, **111**, 2045 (1989).
15) G. Grampp and W. Jaenicke, *Ber. Bunsenges. Phys. Chem.*, **95**, 904 (1991).
16) B. A. Kowert, L. Marcoux, and A. J. Bard, *J. Am. Chem. Soc.*, **94**, 5538 (1972).
17) S. F. Nelsen, D. T. Rumack, and M. Meot-Ner (Mautner), *J. Am. Chem. Soc.*, **109**, 1373 (1987).
18) G. E. McManis, R. M. Nielson, A. Gochev, and M. J. Weaver, *J. Am. Chem. Soc.*, **111**, 5533 (1989).
19) M. J. Weaver, *Chem. Rev.*, **92**, 463 (1992).
20) H. Heitele, *Angew. Chem., Int. Ed. Engl.*, **32**, 359 (1993).
21) G. C. Walker, E. Åkesson, A. E. Johnson, N. E. Levinger, and P. F. Barbara, *J. Phys. Chem.*, **96**, 3728 (1992).
22) D. K. Phelps and M. J. Weaver, *J. Phys. Chem.*, **96**, 7187 (1992).
23) S. Wherland, *Coord. Chem. Rev.*, **123**, 169 (1993).
24) R. M. Nielson, J. T. Hupp, and D. I. Yoon, *J. Am. Chem. Soc.*, **117**, 9085 (1995).
25) G. Rauhut and T. Clark, *J. Am. Chem. Soc.*, **115**, 9127 (1993).
26) G. Rauhut and T. Clark, *J. Chem. Soc., Faraday Trans.*, **90**, 1783 (1994).
27) L. Eberson and S. S. Shaik, *J. Am. Chem. Soc.*, **112**, 4484 (1990).
28) G. L. Closs, L. T. Calcaterra, N. J. Green, K. W. Penfield, and J. R. Miller, *J. Phys. Chem.*, **90**, 3673 (1986).
29) A. J. C. Varandas and S. J. Formosinho, *J. Chem. Soc., Faraday Trans. 2*, **82**, 953 (1986).
30) A. J. C. Varandas and S. J. Formosinho, *J. Chem. Soc., Chem. Commun.*, **1986**, 163.
31) S. J. Formosinho, "Theoretical and Computational Models for Organic Chemistry," ed by S. J. Formosinho, I. G. Csizmadia, and L. G. Arnaut, NATO ASI Series, Kluwer, Dordrecht (1991), p. 159.
32) S. J. Formosinho, *J. Chem. Soc., Perkin Trans. 2*, **1988**, 1209.
33) S. J. Formosinho, *Pure Appl. Chem.*, **61**, 891 (1989).
34) L. G. Arnaut and S. J. Formosinho, *J. Mol. Struct. (Theochem.)*, **233**, 209 (1991).
35) L. G. Arnaut, "Molecular Electrochemistry of Inorganic, Bioinorganic and Organometallic Compounds," ed by A. J. L. Pombeiro and J. McCleverty, NATO ASI Series, Kluwer, Dordrecht (1993), p. 207.
36) S. J. Formosinho and L. G. Arnaut, *J. Mol. Struct. (Theochem.)*, **130**, 105 (1994).
37) S. J. Formosinho and L. G. Arnaut, *J. Photochem. Photobiol. A: Chem.*, **82**, 11 (1994).
38) L. G. Arnaut and S. J. Formosinho, *J. Photochem. Photobiol. A: Chem.*, **75**, 1 (1993).

39) M. G. Evans and M. Polanyi, *Trans. Faraday Soc.*, **31**, 875 (1935).
40) M. G. Evans, *Trans. Faraday Soc.*, **35**, 824 (1939).
41) M. Polanyi, *J. Chem. Soc.*, **1937**, 629.
42) D. J. Mitchell, H. B. Schlegel, S. S. Shaik, and S. Wolfe, *Can. J. Chem.*, **63**, 1642 (1985).
43) R. M. Badger, *J. Chem. Phys.*, **1935**, 710 (1935).
44) G. Grampp, M. C. B. L. Shohoji, and B. J. Herold, *Ber. Bunsenges. Phys. Chem.*, **93**, 580 (1989).
45) J. P. Telo and M. C. B. L. Shohoji, *Ber. Bunsenges. Phys. Chem.*, **98**, 172 (1994).
46) J. L. de Boer and A. Vos, *Acta Crystallogr., Sect. B*, **B28**, 835 (1972).
47) S. F. Nelsen, S. C. Blackstock, and K. J. Haller, *Tetrahedron*, **42**, 6101 (1986).
48) A. C. Reddy, D. Danovich, A. Ioffe, and S. Shaik, *J. Chem. Soc., Perkin Trans. 2*, **1995**, 1525.
49) P. Suppan, *Top. Curr. Chem.*, **163**, 95 (1992).
50) G. Grampp and G. Rauhut, *J. Phys. Chem.*, **99**, 1815 (1995).
51) L. G. Arnaut, "Proton Transfer in Hydrogen-Bonded Systems," ed by T. Bountis, Plenum Press, New York (1992), p. 281.
52) J. R. Miller, L. T. Calcaterra, and G. L. Closs, *J. Am. Chem. Soc.*, **106**, 3047 (1984).
53) J. V. Beitz and J. R. Miller, *J. Chem. Phys.*, **71**, 4579 (1979).
54) J. R. Miller, J. V. Beitz, and R. K. Huddleston, *J. Am. Chem. Soc.*, **106**, 5057 (1984).
55) T. Heinis, S. Chowdhury, S. L. Scott, and P. Kebarle, *J. Am. Chem. Soc.*, **110**, 400 (1988).
56) K. D. Jordan and P. D. Burrow, *Chem. Rev.*, **87**, 557 (1987).
57) G. Binnig, H. Rohrer, C. Gerber, and E. Weibel, *Physica*, **109 & 110B**, 2075 (1982).
58) G. Binnig and H. Rohrer, *Angew. Chem., Int. Ed. Engl.*, **26**, 606 (1987).
59) N. Neto, M. Scrocco, and S. Califano, *Spectochim. Acta*, **22**, 1981 (1966).
60) C. L. Dodson and J. F. Graham, *J. Phys. Chem.*, **77**, 2903 (1973).
61) T. Layloff, T. Miller, R. N. Adams, H. Fäh, A. Horsfield, and W. Proctor, *Nature*, **205**, 382 (1965).
62) J. L. Baudor and M. Sanquer, *Acta Crystallogr., Sect. B*, **B39**, 75 (1983).
63) G. Zerbi and S. Sandroni, *Spectrochim. Acta, Part A*, **24A**, 511 (1968).
64) J. Trotter, *Acta Crystallogr.*, **13**, 86 (1960).
65) K. S. Raymond and R. A. Wheeler, *J. Chem. Soc., Faraday Trans.*, **89**, 665 (1993).
66) L. O. Peitilä, K. Palmö, and B. Mannfors, *J. Mol. Spectrosc.*, **116**, 1 (1986).
67) D. M. Chipman and M. F. Prebenda, *J. Phys. Chem.*, **90**, 5557 (1986).
68) J. Trotter, *Acta Crystallogr.*, **12**, 884 (1959).
69) A. Kuwae and K. Machida, *Spectrochim. Acta, Part A*, **35A**, 27 (1979).
70) V. Malatesta, R. Millini, and L. Montanari, *J. Am. Chem. Soc.*, **117**, 6258 (1995).
71) T. J. Kistenmacher, T. J. Enage, A. N. Bloch, and D. O. Cowan, *Acta Crystallogr., Sect. B*, **B32**, 1193 (1982).
72) R. Bozio, A. Girlando, and C. Pecile, *J. Chem. Soc., Faraday Trans. 2*, **71**, 1237 (1975).
73) D. A. Dixon and J. S. Miller, *J. Am. Chem. Soc.*, **109**, 3656 (1987).
74) J. J. Hinkel and J. P. Devlin, *J. Chem. Phys.*, **58**, 4750 (1973).
75) D. R. Lide, *J. Chem. Phys.*, **22**, 1577 (1954).
76) A. Kuwae and K. Machida, *Spectrochim. Acta, Part A*, **35A**, 841 (1979).
77) L. L. Merritt, Jr., and E. D. Schroeder, *Acta Crystallogr.*, **9**, 801 (1956).
78) N. Neto, M. Muniz-Miranda, L. Angeloni, and E. Castellucci, *Spectrochim. Acta, Part A*, **39A**, 97 (1982).
79) I. Ikemoto, G. Katagiri, S. Nishimura, K. Yakushi, and H. Kuroda, *Acta Crystallogr., Sect. B*, **B35**, 2264 (1979).
80) M. Kubinyi, G. Varsányi, and A. Grofcsik, *Spectrochim. Acta, Part A*, **36A**, 265 (1980).
81) E. Ernstbrunner, R. B. Girling, W. E. L. Grossman, E. Mayer, K. P. J. Williams, and R. E. Hester, *J. Raman Spectrosc.*, **10**, 161 (1981).
82) W. Gordy, *J. Chem. Phys.*, **14**, 305 (1946).
83) C. Trinquecoste, M. Rey-Lafon, and M.-T. Forel, *Spectrochim. Acta, Part A*, **30A**, 813 (1974).
84) A. J. Gordon and R. A. Ford, "The Chemist's Companion," John Wiley, New York (1972), pp. 107 and 114.
85) S. Ghoshal, T. Lu, Q. Feng, and T. M. Cotton, *Spectrochim. Acta, Part A*, **44A**, 651 (1988).
86) R. O. Loutfy and R. O. Loutfy, *Can. J. Chem.*, **54**, 1454 (1976).
87) B. Paulson, K. Pramod, P. Eaton, G. Closs, and J. R. Miller, *J. Phys. Chem.*, **97**, 13042 (1993).
88) H. Oevering, M. N. Paddon-Row, M. Heppener, A. M. Oliver, E. Cotsaris, J. W. Verhoeven, and N. S. Hush, *J. Am. Chem. Soc.*, **109**, 3258 (1987).
89) E. H. Yonemoto, G. B. Saupe, R. H. Schmehl, S. M. Hubig, R. L. Riley, B. L. Iverson, and T. E. Mallouk, *J. Am. Chem. Soc.*, **116**, 4786 (1994).
90) S. Knapp, T. G. Murali Dhar, J. Albaneze, S. Gentemann, J. A. Potenza, D. Holten, and H. J. Schugar, *J. Am. Chem. Soc.*, **113**, 4010 (1991).
91) B. A. Leland, A. D. Joran, P. M. Felker, J. J. Hopfield, A. H. Zewail, and P. B. Dervan, *J. Phys. Chem.*, **89**, 5571 (1985).